

## Geomorphic controls on regional base flow

Marco Marani

Dipartimento di Ingegneria Idraulica, Marittima e Geotecnica, Università di Padova, Padua, Italy

Elfatih Eltahir

Department of Civil and Environmental Engineering and Ralph M. Parsons Laboratory  
Massachusetts Institute of Technology, Cambridge, Massachusetts, USA

Andrea Rinaldo<sup>1</sup>

Dipartimento di Ingegneria Idraulica, Marittima e Geotecnica, Università di Padova, Padua, Italy

**Abstract.** The subsurface hydrological response plays an important role in the hydrology of humid regions. In particular, the physical relationship between base flow dynamics and the fluctuations in spatially averaged water table depth, as described by the groundwater rating curve, determine to a significant extent the nature of statistical persistence of hydrological anomalies in the unconfined aquifers level and river flow. In this paper, we propose that the scale and shape of the groundwater rating curve reflect some of the geomorphological characteristics of the region such as relief, drainage density, and the hypsometric distribution of the elevation field. These connections between geomorphology and hydrology of river basins are investigated using a simple model of unconfined groundwater flow applied to synthetic basins as well as observed basins from Illinois.

### 1. Introduction

The relationship between the hydrologic response and the geomorphologic structure of its river basin has been an active subject for research in hydrology during the last 2 decades. *Rodriguez-Iturbe and Valdes* [1979] developed a theory for linking the surface hydrologic response to geomorphological parameters of a basin. They used the classical unit hydrograph concept to describe the hydrologic response and Horton numbers, as well as other parameters, to describe the geomorphologic structure of a basin. Their pioneering study was followed by several other similar studies on the links between hydrologic processes and basin morphology [e.g., *Gupta et al.*, 1980; *Rodriguez-Iturbe et al.*, 1982; *Kirshen and Bras*, 1983; *Troutman and Karlinger*, 1985; *Rinaldo et al.*, 1991] [see also *Bras*, 1990, chapter 12; *Rodriguez-Iturbe and Rinaldo*, 1997, chapter VII]. In essence, it is now acknowledged that the hydrologic response to intense, flood-producing rainfall events bears the signatures of the geomorphic structure of the channel network and of the characteristic hillslope lengths defining the drainage density of the basin. The interpretation of the hydrologic response as the travel time distribution of a water particle randomly injected in a distributed manner across the landscape inspired many geomorphic insights, including a discussion of the relative role of variance-producing arrival mechanisms [*Rinaldo et al.*, 1991; *Snell and Sivapalan*, 1994] suggesting that geomorphological dispersion, i.e., geomorphically explained variances, are the dominant processes under the general operating conditions for basin dynamics. The interpretation of

the basin width function as the idealized hydrologic response under rather simplified dynamic assumptions [*Kirkby*, 1976] paved the way to more realistic approaches, still dwelling on geomorphic controls although modified by a weighted balance of hillslope and channel pathways yielding a modified width function [*Rinaldo et al.*, 1995]. It is now clear that geomorphic controls are dominant factors that shape the surface hydrologic response of a river basin. We wonder whether the general idea of the controlling role of land morphology also applies to some extent to the regional scales (i.e., relating to areas larger than roughly  $10^4$  km<sup>2</sup>) and to base flows rather than surface responses alone.

In this paper, we are interested in studying the relationship between the long-term average water table depth, the average recharge to the groundwater, and the geomorphology of a basin.

This general topic is theoretically important and deserves significant attention. We are motivated by several observations that document a significant degree of nonlinearity in observed groundwater rating curves [e.g., *Lizarraga*, 1978; *Rasmussen and Anderasen*, 1959; *Schicht and Walton*, 1961; *Senn*, 1980; *Duffy*, 1996; *Eltahir and Yeh*, 1999], that is, in the functions relating mean water table depth to the flux taking place from the aquifer to the streams. A nonlinear groundwater rating curve is found for single hillslopes in upland catchments [*Duffy*, 1996], in agricultural drainage systems with an essentially flat topography [*Senn*, 1980], as well as in larger-scale, more varied, topographies [*Eltahir and Yeh*, 1999]. We focus here on large-scale topographies, and we hypothesize that the interaction between the land surface morphology and the fluctuations in average aquifer water level is a key factor in dictating the observed nonlinear shape [e.g., *Eltahir and Yeh*, 1999] of groundwater rating curves.

In a recent observational study, *Yeh et al.* [1998] described the seasonal and interannual variability in the regional hydrological cycle in Illinois. This is a humid region where the

<sup>1</sup>Also at Ralph M. Parsons Laboratory, Massachusetts Institute of Technology, Cambridge, Massachusetts, USA.

Copyright 2001 by the American Geophysical Union.

Paper number 2000WR000119.  
0043-1397/01/2000WR000119\$09.00

groundwater table fluctuates at  $\sim 2\text{--}4$  m below the surface. Most of the runoff in Illinois is supplied by the discharge from unconfined aquifers into the streams, which was evident in the close association of the dynamics in aquifer level and streamflow. At the timescale of months the regional hydrological cycle in this area reflects the variability in incoming solar radiation, with both aquifer level and river flow responding closely to the seasonal solar cycle. However, at the interannual timescale the story is different: Variability in precipitation is the main forcing of the hydrological floods and droughts that propagate from the atmosphere into the soil and down to the aquifers. *Eltahir and Yeh* [1999] documented a significant asymmetry in the response of aquifers to floods and droughts. While aquifers in Illinois enhance and prolong atmospheric droughts, they tend to dissipate and shorten the duration of atmospheric floods. The explanation of this interesting phenomenon lies in the nonlinear form of the groundwater rating curve. The slope of this rating curve during flood conditions is significantly larger than the corresponding slope during drought conditions. During floods the discharge to streams increases rapidly with the increase in aquifer level which works to reduce the storage quickly and hence dissipate the flood condition. However, during droughts the discharge to streams remains small and does not decrease significantly in response to any decrease in aquifer level. As a result, the water level remains low, and the aquifer system has to wait for the occurrence of a wet episode driven by atmospheric processes in order to bring the aquifer level back to normal conditions. These dynamics have been reflected in the observed persistence patterns of droughts and floods in the average aquifer level and stream flow.

The important role of the groundwater rating curve in explaining the persistence patterns of floods and droughts in Illinois motivates our interest in exploring the physical factors behind observed rating curves. In general, we recognize several factors that are potentially important, chiefly: climate, soil, topography, and land use. We will not discuss here the role of the latter as we are not interested in changes induced by anthropic activities, but we are interested in the relevant hydrologic processes. Soil hydraulic properties and soil depth are always important in dictating the dynamics of any flow in the porous media of groundwater aquifers. Under dry climatic conditions the aquifer level is likely to be so deep such that the discharge from aquifers to streams would not be a significant hydrologic process. However, for relatively humid climates the aquifer level would be high enough such that it intersects with the land surface at the relatively low valleys around the river network. Under those conditions the geomorphological characteristics of the land surface are likely to play a significant role in shaping the interaction between the aquifer and the surface. It is precisely this dynamic interaction that represents the focus of this paper.

## 2. Theoretical Basis for Nonlinear Groundwater Rating Curves

*Eltahir and Yeh* [1999] have discussed the physical basis for nonlinearities in the regional groundwater rating curve (i.e., a regional base flow versus mean depth of the water table) on the basis of an idealized aquifer structure (homogeneous, unconfined, bounded by horizontal impermeable layer, drained by a fully penetrating drainage stream). The basic behavior of the idealized model emphasized important facts, in particular, the

main physical factors that are likely to affect the form of the rating curve. In agreement with previous reports by *Troch et al.* [1993] the base flow discharge, say,  $q$ , drained by a channel of length  $L$ , is determined by the hydraulic conductivity  $K$ , the average elevation of the aquifer over the impermeable level, say,  $\bar{h}$ , and the drainage density  $D$ , meant as a measure of the total length of draining channels per unit area. The dynamics of the base flow in this model reflects the characteristic fluctuations in the aquifer levels and a constant density, in space and time, of the draining boundaries, therefore implicitly assuming that the characteristic horizontal subsurface path of base flow is constant at regional scales. We therefore wonder whether relaxing some of the constraining assumptions above, in particular concerning the description of possible geomorphic controls owing to topographic information which can be easily accessed and objectively manipulated [*Dietrich et al.*, 1992, 1993; *Dietrich and Dunne*, 1993; *Montgomery and Dietrich*, 1988, 1992; *Moore et al.*, 1988a, 1988b; *Rodriguez-Iturbe and Rinaldo*, 1997], will yield further insight into the governing processes.

The first assumption that seems reasonable is that groundwater flow obeys Darcy's law and is essentially horizontal at the regional scales [e.g., *Dagan*, 1989]. Whereas the thickness of the aquifers is usually in the range  $10^0\text{--}10^2$  m, the planar dimension is typically of the order of  $10^3\text{--}10^6$  m, and in quite a few cases we are, indeed, interested in investigating the behavior of the formation as a whole unit, that is, to compute the water head fluctuations caused by recharge applied to the entire aquifer. In such a case the ratio between planar and vertical dimensions is so large that the hydraulic approach (i.e., of planar flow) is surely appropriate. In this approach, water heads and hydraulic conductivity are averaged over the aquifer depth, and they become functions of the planar vector  $\mathbf{x} = (x, y)$  and, possibly, time. In many cases of practical interest the time dependence may be dropped, and a groundwater rating curve is generated by a sequence of steady states. Thus a two-dimensional representation is deemed appropriate at the scales of interest to this paper, implying that much lesser change is experienced in head or specific discharge with depth than over the horizontal domains of interest. Thus the pertinent intrinsic property is the regional transmissivity  $T$  [ $L^2 T^{-1}$ ].

Regional basins experience rather large fluctuations in groundwater drainage density in space and time. In fact, while the usual definition of drainage density addresses the position of the channel heads [*Dietrich et al.*, 1992, 1993; *Dietrich and Dunne*, 1993] which is known to fluctuate as a response to climatic changes [e.g., *Rinaldo et al.*, 1995; *Tucker and Slingerland*, 1997], the fluctuation of the seepage face determining the position of the boundary condition (where the head equals the topographic surface) depends chiefly on geomorphic controls [*Dunne*, 1978; *Duffy et al.*, 1991]. Indeed, the saturation of concave regions [e.g., *Dunne*, 1978] is quite sensitive to geomorphic features like valley density (the length of concave sites, channeled or not, per unit basin area) and recharge rates. Unchanneled valleys bear important geomorphic signatures of climate changes [*Rinaldo et al.*, 1995], but what really matters for determining the groundwater rating curve is the mean distances to (and the relative elevations of) topographically concave sites. Thus valley, rather than drainage, density is the geomorphic feature that controls base flow rating curves in the suggested connection [*Eltahir and Yeh*, 1999]: Rise in mean aquifer depth leads to enhancement of the density of ground-

water drainage which leads to an increase in base flow (of course, the increase in base flow is, in practice, bounded from above by the value of the climatic limit on recharge). In this sense we deem that the relationship between base flow and mean water table depth must be heavily affected by those geomorphic controls that determine the characteristic spatial scales (vertical and horizontal) for the relevant landscape evolution processes.

While typically one looks at sources of variability in the heterogeneous structure of the field of transmissivity (which under common assumptions [e.g., Dagan, 1989] becomes a stationary two-dimensional random function), we wonder whether the variability imposed on boundary conditions by geomorphic controls (i.e., the sequence of valleys and hillslopes of generating runoff areas that control the seepage boundary condition) could dominate base flow production. Heterogeneity prevailing in natural porous formations can be characterized by the order of magnitude of the correlation scales characterizing spatial variability of aquifer transmissivity [Dagan, 1986; Gelhar, 1993], and these, at regional scales, typically vary on the order of hundreds to thousands of meters. Much smaller, instead, at least in humid climates is the characteristic distance one has to walk before encountering a channel, i.e., the inverse of drainage density, typically from tens to a few hundred meters. Since the channel head and the drainage structure work as sinks for the groundwater flow, we assume that it is this “geomorphic” heterogeneity, jointly with a measure of the vertical variability of the drainage surface, that controls regional base flow. Needless to say, it would be of no particular theoretical or practical difficulty to add spatial heterogeneity to the transmissivity field and measure the impact on regional base flow. At this point, however, it seemed more interesting to explore the effects (that, as stated, we deem dominant) of geomorphic and topographic controls.

In the chosen framework therefore the groundwater flow is driven by gradients of head  $\nabla h(\mathbf{x})$ , possibly limited by the topographic gradients  $\nabla z(\mathbf{x})$ , where  $h(\mathbf{x})$  is the water table elevation and  $z(\mathbf{x})$  is the topographic elevation. The latter is easily accessible, even at regional scales, in discretized lattices through digital elevation maps (DEMs) (e.g., see Rodriguez-Iturbe and Rinaldo [1997] for an in-depth discussion). We assume, in agreement with common assumptions, that fluctuations in the water table are much smaller than the overall mean depth of the regional aquifer and that the integration of the permeability field produces a meaningful average transmissivity value (i.e., that the mean value computed from a sample does not depend on the size of the sample itself because of a power law form of the transmissivity probability distribution [e.g., see Dagan [1994]]).

If  $r$  is a conventional net recharge term, uniformly distributed in space and time, and  $T$  is the reference regional transmissivity, the basic continuity equation becomes a Poissonian problem:

$$\nabla^2 h = -\frac{r}{T} = -c. \quad (1)$$

Boundary conditions are the key factor, and they will be discussed in detail in section 3.

Clearly, other options are possible. Another modeling option is to assume the impermeable layer on which the aquifer rests to be approximately horizontal [Dagan, 1989] and to solve the nonlinear problem

$$\nabla^2 h^2 = -2r/K. \quad (2)$$

Here  $K$  would be the “regional” hydraulic conductivity [ $L T^{-1}$ ].

The above approach (equation (1)) may account for spatial heterogeneity through a suitable definition of a random space function  $T(\mathbf{x})$ , possibly lognormal [Dagan, 1989]. The relevant stochastic boundary value problem would become, in terms of a first-order perturbation analysis valid for relatively low variances of the log transmissivity values,  $\nabla^2 h = -r/\langle T \rangle + \nabla Y \cdot \nabla h/\langle T \rangle$ , where  $Y$  is a stationary Gaussian field ( $T(\mathbf{x}) = \langle T \rangle e^{Y(\mathbf{x})}$ ). The basic structure of the mathematical problem (1) would then be retained except for large variance of the transmissivity field and/or for very small integral scales of the field  $T(\mathbf{x})$ . Both conditions are similarly of lesser relevance to regional scales [Dagan, 1989, chapter 5; Gelhar, 1993] therefore suggesting that formulation (1) appropriately describes the problem of interest. Thus in the ensuing computations we will retain the basic forms (1) or, alternatively, (2) of the boundary value problem.

### 3. Numerical Procedures and Results: Nonlinear Groundwater Rating Curves

A DEM from the United States Geological Survey for a part of the state of Illinois was used to test the model formulated in section 2. The DEM used has a grid resolution of 90 m and a grid extent of 63 km by 63 km.

Equation (1) was discretized with a forward finite difference method [e.g., Abramowitz and Stegun, 1964], which yields, for given values of recharge and transmissivity, a set of simultaneous linear equations with a symmetric, positive-definite matrix. In order for the problem to be well posed, a set of boundary conditions needs to be specified. Two types of boundaries may be distinguished: the boundary constituted by those locations where the groundwater surface  $h(\mathbf{x})$  crosses the ground surface  $z(\mathbf{x})$ , i.e., the saturated sites, and the outer boundary of the computation domain, where the condition imposed by the surrounding groundwater system must be prescribed.

Let us first discuss the boundary conditions to be imposed on saturated sites. The problem is that of dealing with the points where the value  $h(\mathbf{x})$  of the groundwater surface would exceed the elevation of the ground  $z(\mathbf{x})$  when just the boundary condition on the outer boundary is imposed. At those locations, belonging to channels and valleys, surface flow occurs for the given forcing  $c$  (units  $L T^{-1}$ ). These points thus belong to the boundary of the integration domain for (1), and there a boundary condition on the value of  $h(\mathbf{x})$  must be prescribed. To identify the sites belonging to this type of boundary, for a given value of  $r$  (note that  $T$  is fixed and that its numerical value is immaterial to the analysis), (1) is first solved for a succession of increasing values  $0 < r_1 < r_2 < \dots < r_i < \dots < r$ . For the  $i$ th value  $r_i$  the pixels  $\hat{\mathbf{x}}_k$ , where  $h(\hat{\mathbf{x}}_k) \geq z(\hat{\mathbf{x}}_k)$ , are identified and included in the boundary. The condition  $h(\hat{\mathbf{x}}_k) = z(\hat{\mathbf{x}}_k)$  (neglecting the contribution to the hydraulic head because of the presence of a sheet of water on the surface of the ground) is then imposed when solving (1) for the following value  $r_{i+1} > r_i$ . As the value  $r_i$  of the recharge increases in steps  $\Delta r$  to the value  $r$ , all the locations where streamflow takes place are in this manner identified. To ensure robustness, the sensitivity of the solution to the value  $\Delta r$  was explored and a value  $\Delta r_0$  below which the solution did not change was adopted.

Let us now address the problem of assigning a boundary

condition on the outer boundary of the computation grid. It is clear that the choice of the boundary conditions is somewhat arbitrary and has an impact on the solution, at least in the proximity of the outer boundary. It should be pointed out that a no-flux boundary condition, which has the advantage of not imposing an arbitrary elevation value to the groundwater surface, does not seem to be appropriate since it would a priori force a balance between recharge and streamflow. This would constitute a constraint for the system which would not be allowed to partly dissipate recharge to the groundwater through flux across the outer boundary of the domain. To avoid this problem and to minimize spurious effects on the characters of the solution, the groundwater surface in the domain is assumed to be globally in equilibrium with the surrounding (outside the domain) groundwater system. It is, in fact, assumed that the groundwater surface inside and outside the domain have the same, unknown, average elevation, which is used as a boundary condition. Since the average elevation is unknown, an iterative procedure is necessary in order to impose the correct boundary condition. The discretized Poisson equation is thus solved by imposing a tentative boundary condition, for example, chosen as the minimum elevation of the topography in the entire domain. Once the solution is found, the average elevation of the groundwater surface in the domain is computed. This value is then used as a boundary condition in (1), a new groundwater surface is found, and the new average elevation is computed. The procedure is repeated until two successive values differ by an amount smaller than a fixed tolerance. A detailed description of the numerical procedure used may be found in Appendix A. The boundary condition imposed through this procedure may, in principle, lead to locally imposing to the groundwater surface a level higher than the topographic elevation. This has not been observed in any of the numerical experiments performed, and the potential influence on the solution has been eliminated by discarding from the analyses a buffer zone near the outer boundary as described below.

For varying values  $r$  (or  $c$ , being  $T$  fixed) through the doubly iterative procedure just described, the equilibrium groundwater surface  $h(\mathbf{x})$  together with its mean elevation  $\bar{h}$  and the set of points where saturation occurs, that is, where  $h(\hat{\mathbf{x}}_k) = z(\hat{\mathbf{x}}_k)$ , is thus found.

The (doubly) iterative nature of the procedure described requires an efficient implementation in computing the Poissonian surface  $h(\mathbf{x})$  as this must be done repeatedly at each iterative step. An efficient solution is obtained by using an accelerated conjugate gradient technique [e.g., Marani et al., 1998] coupled to a relaxation scheme which adjusts the solution when boundary conditions are changed slightly in the course of the iterations.

The procedure described above was applied, for different values of the forcing  $c$  at the right-hand side of (1), to a synthetic basin with the same characteristics as natural ones for elevation field structure and network connectivity properties (the basin was obtained through a process of self-organized critical evolution; see Rodriguez-Iturbe and Rinaldo [1997] for reference). The choice of a synthetic basin depended on computational convenience, but tests were performed on a DEM of Illinois of size  $700 \times 700$  pixels as well.

Figure 1 shows the groundwater surface (together with the topography) for the synthetic DEM used and for some of the values of  $r$  explored. It may be seen how the groundwater elevation increases as the value of the recharge is increased.

The water table surface also looks increasingly "rougher" as its elevation is set to the topographic elevation at an increasing number of sites for growing recharge values.

Figure 2 shows the sets of points which become saturated for progressively larger values of the recharge  $r$ . The area of such sets obviously increases with  $r$ .

It is now interesting to relate the total flow to the streams  $q_s$  (units  $L^3 T^{-1}$ ) to the recharge and the character of the topographic surface. The value of  $q_s$  may, in fact, be computed, once  $h(\mathbf{x})$  is known, as the difference between the integral of the recharge  $r$  to the groundwater system over the domain and the integral over the entire boundary (i.e., including both saturated sites and the outer grid boundary)  $q_b$  (units  $L^2 T^{-1}$ ) of the groundwater flux:

$$q_b = T \nabla h \cdot \mathbf{n}, \quad (3)$$

with  $\mathbf{n}$  indicating the outgoing normal to the boundary.

As the recharge is assumed to be uniform over the domain, the total flow to the streams is computed as

$$q_s = Sr - \int_{\partial S} T \nabla h \cdot \mathbf{n} ds, \quad (4)$$

where  $\partial S$  indicates the outer boundary of the domain of area  $S$ .

To avoid the necessity of specifying a value for the transmissivity and to be able to compare results from grids of different extents, (4) is divided by  $T S$ , obtaining streamflow per unit area per unit value of transmissivity  $q'_s$  (units  $L^{-1}$ ). Recalling that (equation (1))  $r/T = c$ ,

$$q'_s = c - \frac{1}{S} \int_{\partial S} \nabla h \cdot \mathbf{n} ds. \quad (5)$$

By applying this procedure to the groundwater surfaces  $h(\mathbf{x})$  corresponding to different values of the forcing  $c$ , one finds a series of values  $(\bar{h}, q'_s)$  thereby obtaining a groundwater rating curve.

The groundwater rating curves for subgrids of the Illinois DEM are given in Figure 3. The subgrids are all centered around the center of the largest  $700 \times 700$  pixel grid, and thus the boundary of the progressively smaller grids is progressively farther from the outer boundary of the domain where the Poisson equation (1) was solved. It is seen that results tend to coincide (particularly for large grids, which have an averaging effect on possible local anomalies) and that all rating curves exhibit the same shape and steepening for increasing values of streamflow. The close agreement observed in the rating curves computed shows that the effect of the boundary conditions on the characters of the solution  $h(\mathbf{x})$  is negligible. In fact, the nonlinear features of the rating curves are very similar for grids including the boundary (the  $700 \times 700$  pixel grid) and for subgrids away from the outer boundary (all the smaller grids). Further, experiments with different, fixed boundary conditions (e.g., no-flux conditions) yielded very similar results, confirming that the analysis is very robust with respect to the type of boundary conditions used. In conclusion, no appreciable effect of the type of condition imposed on the external boundary was found. Nevertheless, to assure the generality of the results, all computations described in the following are performed on subgrids obtained by eliminating a buffer zone close to the

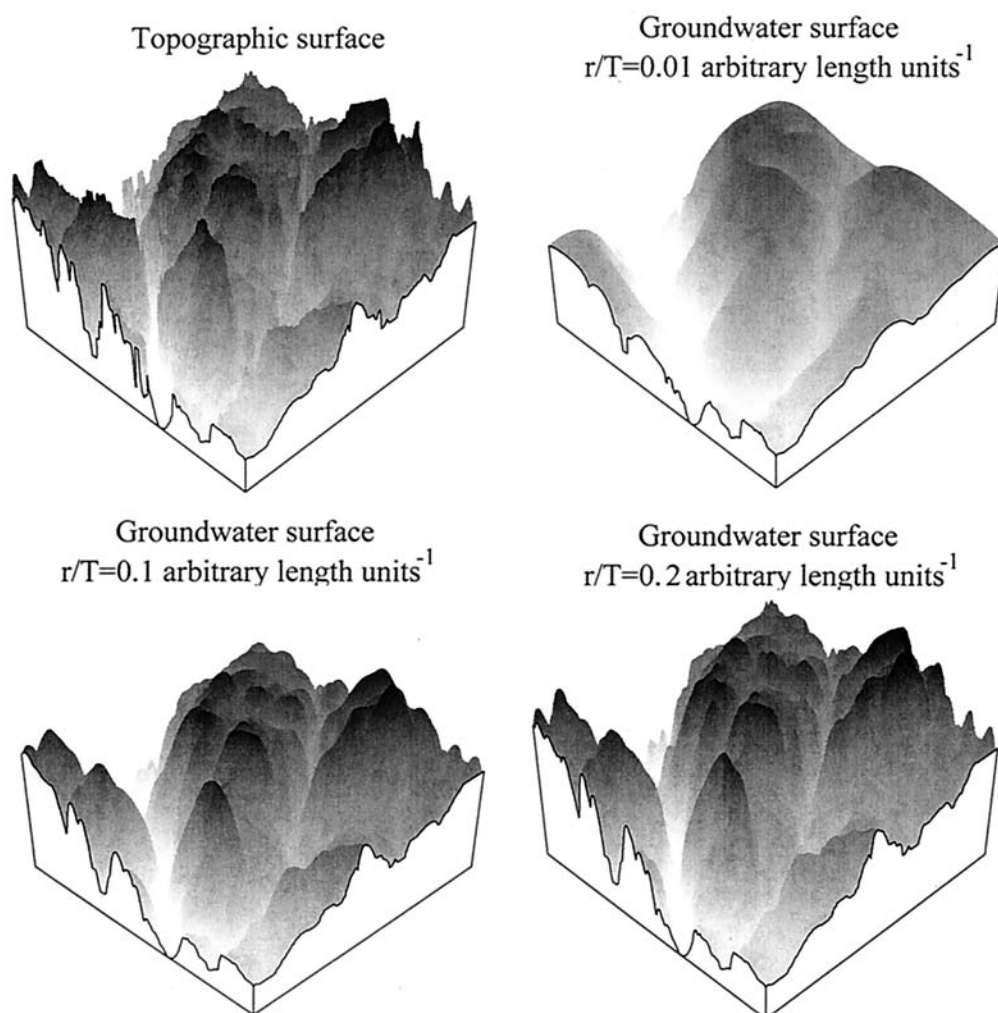


**Figure 1.** Topography of the synthetic basin used and groundwater surface for some of the values of recharge explored.

external boundary whose width was chosen to be one fourth of the domain length.

Finally, a study of the solutions of the formulation given by (2) was also performed. The groundwater rating curves were very similar to the previous case and confirmed the robustness of the nonlinear features observed in Figure 3.

The form of the groundwater rating curve is important. *Eltahir and Yeh [1999]* showed, in fact, that the nonlinearity of the rating curve may explain the fact that aquifer levels are much more sensitive to negative (drought) anomalies than to positive (flood) anomalies. The nonlinearity found in Figure 3 shows that an aquifer is much more efficient in dissipating, through streamflow, the positive anomalies at large values of mean groundwater elevation than in dissipating droughts at low values of  $\bar{h}$ . This nonlinearity stems from the interaction of the groundwater surface with the ground surface as the aquifer intersects more and more of the topography for increasing average elevations  $\bar{h}$ , giving way to a rapidly increasing streamflow. On the other hand, as the elevation of the aquifer decreases, its interaction with the topography becomes weaker and weaker, inducing very little change in the slope of the groundwater rating curve for very low values of  $\bar{h}$ .

The way topography and aquifer interact, for a given average

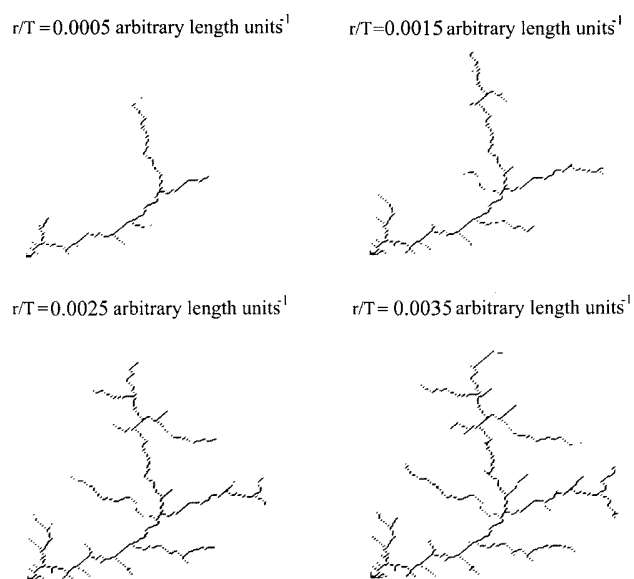


**Figure 2.** Sets of saturated sites for increasing values of the recharge to the groundwater system.

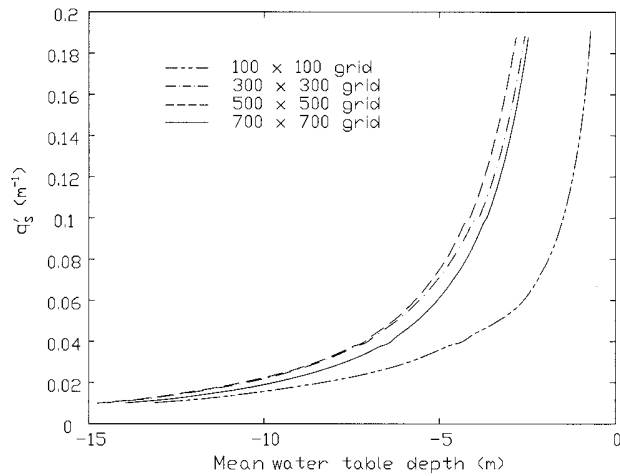


**Figure 3.** Groundwater rating curves for subgrids of varying extents of the Illinois digital elevation map (DEM) computed with the model proposed.

aquifer depth, must be dependent on the characteristics of the topography. A greater interaction between the water table and the ground surface should, in fact, be expected for topographies with larger variances.

This is confirmed by the results in Figure 4 where the rating curve obtained from the synthetic DEM described above are shown. The rating curves in Figure 4 refer to topographies obtained from such a DEM by multiplying its elevations values by a factor  $f$ . By increasing  $f$ , one obtains topographies with larger variance while not changing the form of the probability distribution of elevation values (hypsothetic curve).

It may be seen that for a given water table depth, streamflow is larger for topographies having a larger variance, because of the increased surface “wetted” by the water table. Similarly, for a

given value of the recharge a shallower groundwater elevation is to be expected for topographies exhibiting smaller variance.

Further, it may be observed that the derivative of the recharge with respect to water table depth is larger for topographies with larger variance. This is due to the fact that for a unit decrease of mean water table depth the amount of area which becomes saturated is larger when the variance is large.

It is important to note that performing the same numerical experiments based on formulation (2) rather than (1) yields the same results, further strengthening the robustness of the behavior described.

It is interesting to investigate the influence of the whole probability distribution (hypsothetic curve) of the elevation field on the interaction between topography and groundwater surface. The point is understanding whether, as far as the interaction with the groundwater is concerned, the second moment of the elevation distribution (variance) is enough to characterize the role of the topography. To address the question, we computed the groundwater rating curve, as in Figure 4, for elevation fields characterized by the same value of the variance and different shapes of the hypsothetic curve. In particular, Figure 5 compares the results for two such fields. The first field (dotted line) was obtained by raising the elevation values of the original DEM to a power larger than 1 (we chose the value 1.4). The second field (solid line) was obtained from the same DEM by multiplication by a factor such that the resulting variance was the same as in the previous case. Figure 5 indicates that the value of the variance alone is not sufficient to characterize the role of the topography in determining streamflow and that the shape of hypsothetic curve plays an important part in this respect. In particular, the different forms of groundwater rating curves are determined by the fact that an increase (decrease) in the mean groundwater depth determines the wetting (drying) of a portion of the total area which is different for elevation fields having different hypsothetic curves.

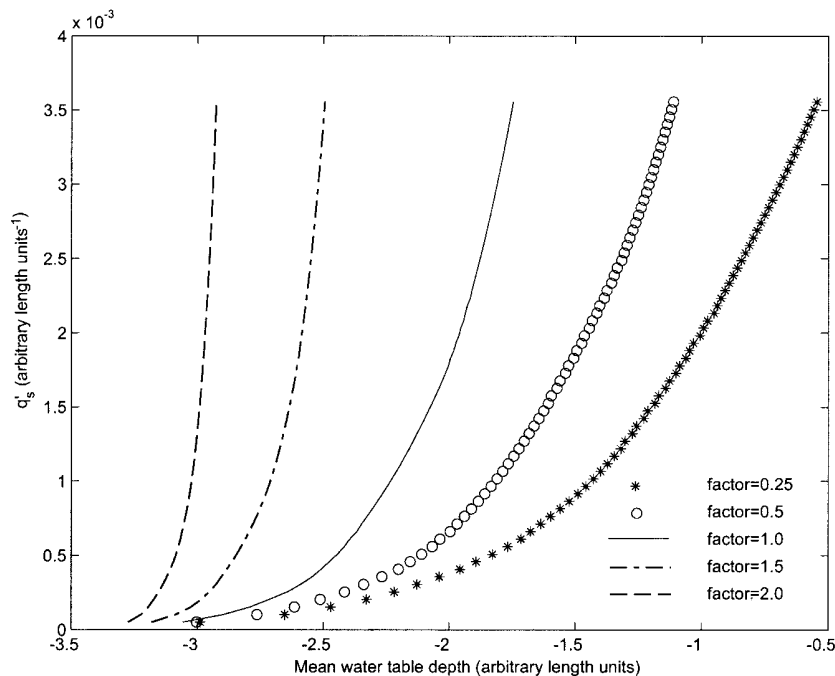


**Figure 4.** Groundwater rating curves computed for synthetic DEMs having different variances.

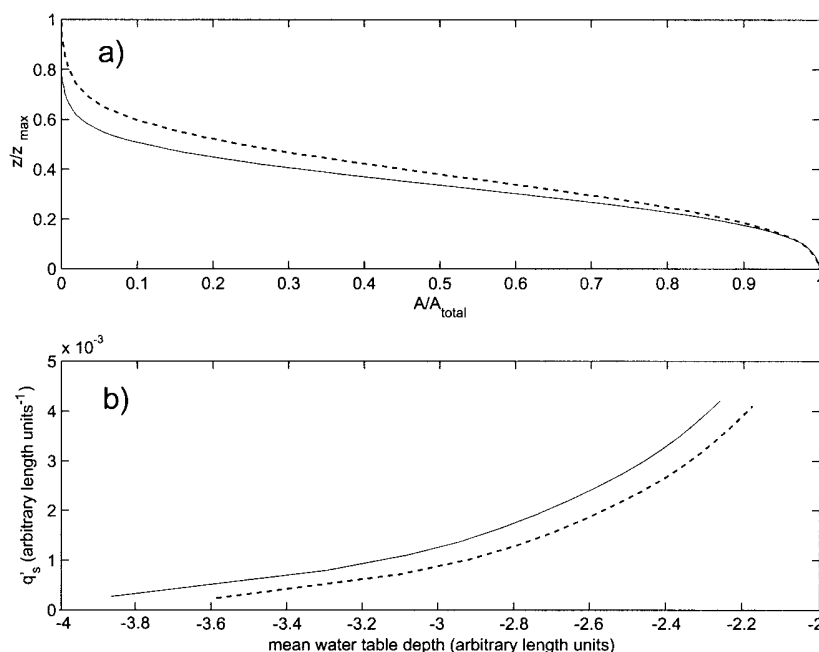


**Figure 5.** Groundwater rating curves computed for (a) different hypsometric curves and (b) synthetic DEMs having the same variance. The DEMs are obtained by elevation to a power (dotted line) or by multiplication by a factor (solid line).

#### 4. Dimensional Analysis

It is interesting to perform a dimensional analysis of the problem in order to identify the controlling parameters and to establish a relationship between them. The results presented in section 3 suggest that the choice of the problem formulation (equations (1) or (2)) will not affect the results of such an analysis in a conceptual manner. The choice of the framework thus becomes a matter of convenience: We chose the more immediate formulation (1).

The dimensional quantities that enter the description of the phenomenon are (see Figure 6) as follows.

1. Here  $q'_s$  is streamflow per unit area and per unit of hydraulic transmissivity ( $L^{-1}$  units). This is the base flow resulting from the interaction between the topography and the groundwater surface. Notice that in a steady state the outgoing flux (base flow plus flux across outer boundary) must equal the

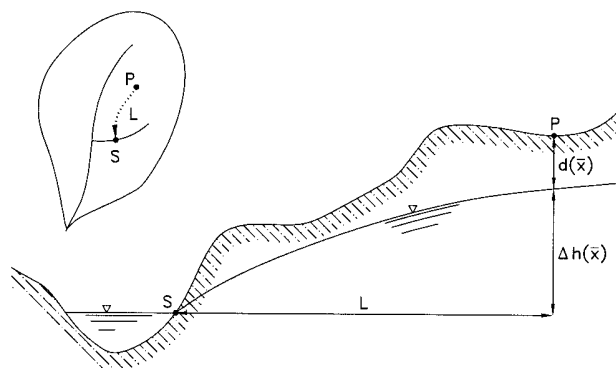


**Figure 6.** Path of a water parcel infiltrating to the groundwater at generic site P and traveling along groundwater surface to the nearest saturated point S.

incoming flux (recharge to the groundwater system by infiltration). Since the flux across the outer boundary tends to become a negligible fraction of the recharge as the size of the domain grows larger, recharge approaches  $q'_s$ .

2.  $\Delta h$  is a characteristic vertical length scale. The discussion of section 3 indicates that topographic variance is not a suitable choice as it is unable to fully capture the interaction between topography and groundwater surface. A relevant vertical scale should embed the influence of both topographic and groundwater surface configuration. Such a length scale may be obtained by considering (see Figure 6) the path that a water parcel deposited at a generic site P must travel in the groundwater to reach the nearest saturated site S (where the parcel exfiltrates into a surface stream) moving in the direction of the steepest descent of the groundwater surface. The elevation difference  $\Delta h(\mathbf{x})$  between site P and site S gives a measure of the potential energy of the parcel, and, for a given velocity of the groundwater, it is related to the discharge per unit area that crosses site P. A global parameter is obtained by computing the mean vertical drop, the spatial average  $\overline{\Delta h}$  of  $\Delta h(\mathbf{x})$ .

3.  $\overline{\Delta h}/L$  is a characteristic energy gradient (nondimensional units). A meaningful energy gradient is obtained by dividing  $\Delta h(\mathbf{x})$  by the length  $L(\mathbf{x})$  of the path from site P to site S. Spatial averaging yields a global parameter.

The variability of the parameters introduced with respect to recharge is shown in Figure 7 for the synthetic DEM used. Several computations have been performed on different DEMs obtained from the basic one, either by multiplying all elevation values by a constant factor or by raising them to a power larger than 1. All the results obtained were consistent with those of Figure 7. It is seen how mean path length  $L$  (Figure 7a, square symbols) decreases for increasing recharge as the saturated areas expand. On the contrary, mean drop  $\overline{\Delta h}$  increases as the forcing at the right-hand side of (1) grows

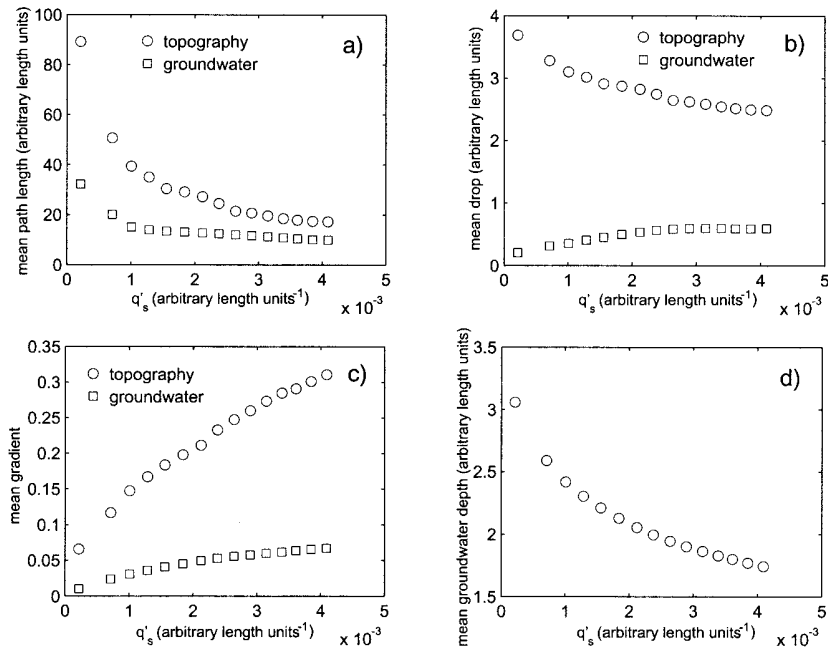


**Figure 7.** Variability of (a) mean path length, (b) mean vertical drop and (c) the resulting values of the mean gradient computed over the groundwater (squares) and the topography (circles) for the reference synthetic DEM of Figure 1. (d) Mean water table depth indicated for reference.

thereby increasing the curvature of  $h$ . The overall effect is an increase of the mean groundwater gradient. Figure 7 also shows the changes in the same quantities, mean vertical drop and energy gradient ( $\Delta z$  and  $\Delta z/L_p$ , respectively), computed with respect to the topographic surface (circles). For their computation the path from the generic point P to the nearest saturated site is determined by moving in the direction of the steepest descent over the topographic surface. The path thus computed is, in general, different from the one determined over the groundwater, with a different vertical drop and a different path length. It is seen in Figure 7a that the mean path length is generally larger over the topography (circles) than on the groundwater surface (squares), as the trajectory is less direct. Mean drop is also larger on the topography than on the groundwater surface (see Figure 6) and decreases for increasing recharge as saturated areas expand. It is also seen that for large values of the recharge the values of mean vertical drop and mean path length tend to stabilize giving a fixed relationship between quantities computed over the topography and those for the groundwater. This suggests the possibility of substituting quantities relative to the groundwater with those, purely geomorphological, computed on the topography.

A geomorphological parameter with important implications for runoff generation is drainage density. It may be formally defined as the inverse of the average path length and is a measure of the extent of the surface drainage network [e.g., Horton, 1945; Rodriguez-Iturbe and Rinaldo, 1997; Tucker *et al.*, 2001]. We may here define the corresponding groundwater parameter, a groundwater drainage density, as the inverse of the mean path length computed over the groundwater surface. The value of groundwater drainage density is a result of the interaction between topography and groundwater, i.e., of the proportion of saturated areas. The mutual dependence of re-

charge and groundwater drainage density is shown in Figure 8, where results for the two DEMs of Figure 5 are shown. Our computations seem to indicate an approximately linear dependence.

Turning back to dimensional analysis, the three quantities introduced above depend on just one fundamental unit: length. Thus, according to dimensional analysis theory [Buckingham, 1914; Langhaar, 1951] the phenomenon may be described through a function involving two nondimensional ratios. We choose:  $\Delta h/L$  and  $q'_s \Delta h$ .

The governing equation thus has the following form:

$$q'_s \overline{\Delta h} = f(\overline{\Delta h/L}). \quad (6)$$

The form of (6) may be found from data or through numerical simulation, and its knowledge allows, with knowledge of  $\overline{\Delta h}$  and  $\overline{\Delta h/L}$ , an estimate of the recharge to base flow for a given area.

Figure 9 shows the results of computations performed on the synthetic DEM described in section 3. The nondimensional groundwater rating curves shown were obtained as follows. The procedure described in the previous paragraphs was applied to solve (1). The solution allows, for fixed values of the recharge, the determination of  $\overline{\Delta h}$ ,  $\overline{\Delta h/L}$ , and  $q'_s$  on the basis of the computed groundwater surface and thus the determination of a couple of nondimensional values ( $q'_s \overline{\Delta h}$ , and  $\overline{\Delta h/L}$ ). By varying the value of the input recharge, a set of such couples is determined. To test the correctness of the dimensional analysis performed, one must now compute the sets of values ( $q'_s \overline{\Delta h}$ , and  $\overline{\Delta h/L}$ ) resulting from the solution of the Poisson problem (1) applied to elevation fields with different topographic characters. These fields were obtained both by multiplying the elevation values by factors (circles in Figure 9, factors ranging from 1 to  $\sim 7$ ) and by raising the elevation values to different exponents (stars in Figure 9, exponents ranging from 1 to 2)

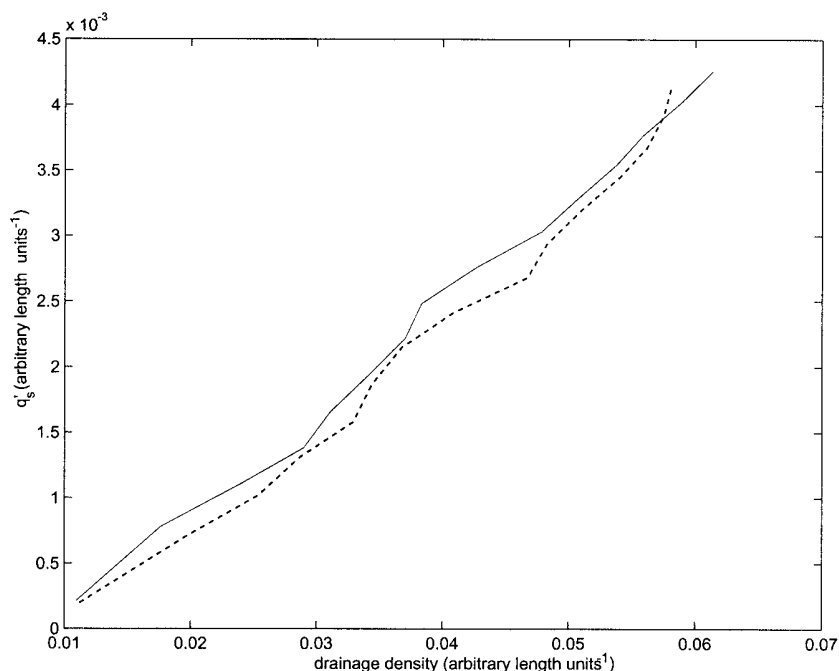


**Figure 8.** Mutual dependence of streamflow and groundwater drainage density for DEMs with the same standard deviation (3.03 arbitrary length units), obtained by raising the values of the same DEM to a power (dotted line, exponent equal to 1.4) or by multiplying them by a suitable factor (solid line, factor equal to 2.31).

thus changing both the probability distribution and the correlation structure of the elevation field.

The results in Figure 9 show quite a consistent collapse of the numerical values on a single curve, suggesting that the

parameters used in the dimensional analysis are correctly describing the behavior of the system even when the statistical characteristics of the topography are radically changed.

The relationship shown in Figure 9 is very interesting and may

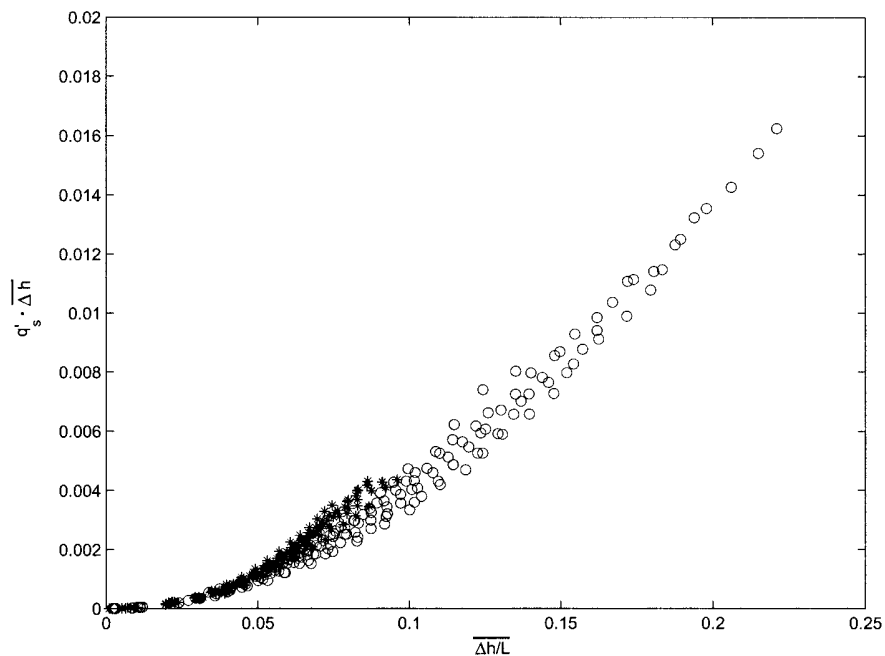


**Figure 9.** Nondimensional groundwater rating curves obtained through numerical computations. The mean water drop and path length are computed over the groundwater surface. The circles indicate results from DEMs obtained from the original by multiplication by constant factors (11 values ranging from 1.00 to 7.43). The stars indicate results from DEMs obtained by raising the original elevation values to different powers (11 values ranging from 1.00 to 2.00).

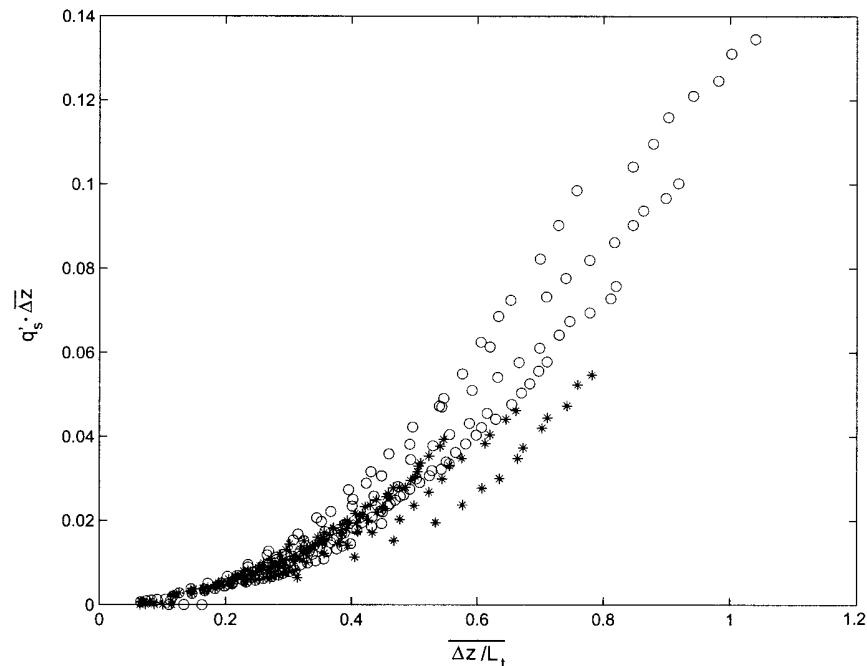


**Figure 10.** Nondimensional groundwater rating curves obtained through numerical computations. The mean water drop and path length are computed over the topographic surface. The circles indicate results from DEMs obtained from the original by multiplication by constant factors. The stars indicate results from DEMs obtained by raising the original elevation values to different powers.

be useful in applications, for example, to estimate base flow from a hydrological basin for which topography and average transmissivity are known. Such an estimate requires the implementation of the model described above to determine the values of the parameters  $\overline{\Delta h}$  and  $\overline{\Delta h/L}$  for use in relationship (6).

It is interesting to investigate the possibility of substituting the parameters relative to the groundwater with parameters of a purely geomorphic nature characterizing the topography. Figures 7a and 7b suggest that there tends to be, at least for large values of the recharge, a fixed relationship between the mean vertical drop and path length computed over the groundwater surface and the topographic surface as all these quantities tend to constant values. This suggests that, at least in this regime, the parameters relative to the groundwater may be substituted by those relative to the topographic surface with a good degree of approximation. Figure 10 shows how the nondimensional groundwater rating curve changes when properties computed over the topography ( $\Delta z$  and  $\Delta z/L_t$ ) are used to give the following relation:

$$q_s' \overline{\Delta z} = f(\overline{\Delta h/L_t}). \quad (7)$$

It is seen that the collapse of results obtained from DEMs with different topographic properties is less robust than in Figure 9. This is to be expected as  $\overline{\Delta z}$  and  $\overline{\Delta h/L_t}$  are only proxies for  $\overline{\Delta h}$  and  $\overline{\Delta h/L}$  which are the real controlling parameters. Nevertheless, the relationship in Figure 10 is useful as it only involves geomorphic quantities directly derivable from a digital model of a basin and is therefore of straightforward application.

## 5. Conclusions

A simple, yet conceptually sound model, based on the application on a regional scale of the Poisson equation has been

developed. The model allowed the exploration of the interaction between topography and groundwater and the clarification of the nonlinear nature of the groundwater rating curve previously observed and justified on other grounds [Eltahir and Yeh, 1999]. In particular, it has been shown that such nonlinearity arises from the nonlinear dependence on the water table depth of the extent of the area through which seepage from the groundwater into the drainage network may occur. In fact, as the depth to the water table decreases, more and more of the troughs may intersect it and thus enhance flow to the drainage network. This observation explains the reason for the more-than-linear increase of base flow recharge with an increasingly shallower water table. However, when the groundwater surface is deeper, the interface area through which seepage can occur decreases sharply yielding a more-than-linearly decreasing recharge to the base flow. This behavior explains the observation [Eltahir and Yeh, 1999] that upward fluctuations of the water table are efficiently damped by the groundwater system, while downward fluctuation show a much larger persistence.

Our results may be interpreted by considering the degree of nonlinearity dependent on how fast the amount of area of a topography below a threshold level decreases when the threshold is decreased. Therefore the controlling factor here is the probability distribution of area with elevation or the hypsometric curve. In particular, distributions with longer tails (i.e., with a large proportion of “low” areas) will produce a relatively larger interaction with the groundwater when this is relatively deep. This effect may be related to the variance of the elevation field, and it was shown how large variances give, for a fixed value of the water table depth, a larger recharge to base flow (or, alternatively, for a fixed value of the recharge to base flow a deeper water table). Furthermore, it was seen that topographies with larger variances yield groundwater rating curves

with larger sensitivity to water table depth, and thus they are more efficient in dissipating upward fluctuations of the water table.

Finally, a conceptual framework was developed, based on dimensional analysis, to identify the factors governing the interaction between topography and groundwater. A relationship (equation (6)) was found involving two nondimensional parameters. A first parameter,  $\Delta h/L$ , is the average ratio between horizontal and vertical characteristic lengths and expresses the magnitude of the groundwater surface gradients. Another parameter,  $q'_s \Delta h$ , introduces the dependence from the groundwater level and brings base flow into play. The form of the nondimensional groundwater rating curves thus introduced was found numerically (Figure 9), confirming the correctness of the dimensional analysis approach used. The curves in Figure 9 constitute a tool for estimating base flow from quantities which may be obtained by applying the approach presented to a DEM. It was finally shown that when the groundwater parameters in (6) are substituted with their topographic counterparts, a different nondimensional relationship is found, which, nevertheless, satisfactorily describes the behavior of widely different topographies (in terms of the form of the elevation probability distribution). This approach has the advantage of substituting the characteristics of the groundwater table, which may be determined only through complex measurements or numerical computation, with those of the topography, which may be obtained from commonly available DEMs in a straightforward manner.

## Appendix A

This appendix describes in detail the algorithmic approach adopted to determine the groundwater surface for different values of the forcing term  $c$  in (1). Notice that since the results are normalized by the value of transmissivity, the determination of the groundwater surface is performed for a unit value of  $T$ , which implies the numerical equality of the values of  $r$  and  $c$ .

Algorithm steps are as follows.

1. Do 13. Set  $c$  equal to  $c_{\min}$ ,  $c_{\max}$ . (Loop over values of the forcing.)
2. On the outer boundary, set  $h(\mathbf{x}_{\text{out}})$  equal to the minimum value of  $z(\mathbf{x})$ . (Initialize the boundary condition to an arbitrary low value.)
3. Do 7. Set  $c'$  equal to  $c_{\min}/10$ ,  $c$ ,  $dc$ . (Increase the forcing to the current value  $c$  by steps  $dc$  to determine the saturated sites.)
4. Solve (1) with  $c'$  to determine the groundwater surface  $h(\mathbf{x})$ .
5. Loop over the domain to find locations  $\hat{x}_k$ , where  $z(\hat{x}_k) \leq h(\hat{x}_k)$ .
6. If at least one  $\hat{x}_k$  is found, include all locations  $\hat{x}_k$  in the boundary conditions where it is set  $z(\hat{x}_k) = h(\hat{x}_k)$  and go to step 4. If no new saturated location is found continue to step 7.
7. End do. (The saturated sites have been found together with the groundwater surface.)
8. Compute new mean value  $\bar{h}$  of the groundwater surface  $h(\mathbf{x})$ .
9. If the difference  $\Delta \bar{h}$  between the new mean value and the previous one is larger than a fixed tolerance, then set new outer boundary conditions  $h(\mathbf{x}_{\text{out}}) = \bar{h}$  and go to step 3. Else, if  $\Delta \bar{h}$  is smaller than the tolerance, continue to step 10.
10. Compute the mean water table depth  $\bar{d}$ , that is, the

mean of  $d = h(\mathbf{x}) - z(\mathbf{x})$  over a subgrid which excludes a buffer zone near the outer boundary. (This minimizes the effects of outer boundary conditions.)

11. Compute the flux across the outer boundary of the Subgrid to compute  $q'_s$  in equation (5).
12. Write to disk the values of  $q'_s$  and  $\bar{d}$ .
13. End do. (This is where the loop on the values of the forcing ends.)
14. Stop.

## References

- Abramowitz, M., and I. A. Stegun (Eds.), *Handbook of Mathematical Functions With Formulas, Graphs, and Mathematical Tables*, U.S. Govt. Print. Off., Washington, D. C., 1964.
- Bras, R. L., *Hydrology: An Introduction to Hydrologic Science*, Addison-Wesley-Longman, Reading, Mass., 1990.
- Buckingham, E., On physically similar systems: Illustrations of the use of dimensional equations, *Phys. Rev.*, 4, 345–364, 1914.
- Dagan, G., Statistical theory of groundwater flow and transport: Pore to laboratory, laboratory to formation, and formation to regional scale, *Water Resour. Res.*, 22, 120S–134S, 1986.
- Dagan, G., *Flow and Transport in Porous Formations*, Springer-Verlag, New York, 1989.
- Dagan, G., The significance of heterogeneity of evolving scales to transport in porous formations, *Water Resour. Res.*, 30, 3327–3336, 1994.
- Dietrich, W. E., and T. Dunne, The channel head, in *Channel Network Hydrology*, edited by K. Beven and M. J. Kirkby, pp. 175–219, John Wiley, New York, 1993.
- Dietrich, W. E., C. J. Wilson, D. R. Montgomery, J. McKean, and R. Bauer, Erosion thresholds and land surface morphology, *Geology*, 20, 675–679, 1992.
- Dietrich, W. E., C. J. Wilson, D. R. Montgomery, and J. McKean, Analysis of erosion thresholds, channel networks, and landscape morphology using a digital terrain model, *J. Geol.*, 101, 259–278, 1993.
- Duffy, C. J., A two-state integral-balance model for soil moisture and groundwater dynamics in complex terrain, *Water Resour. Res.*, 32, 2421–2434, 1996.
- Duffy, C. J., K. Cooley, N. Mock, and D. H. Lee, Self-affine scaling and subsurface response to snowmelt in steep terrain, *J. Hydrol.*, 123, 395–414, 1991.
- Dunne, T., Field studies of hillslope flow processes, in *Hillslope Hydrology*, edited by M. J. Kirkby, pp. 227–293, John Wiley, New York, 1978.
- Eltahir, E. A. B., and P. J.-F. Yeh, On the asymmetric response of aquifer water level to floods and droughts in Illinois, *Water Resour. Res.*, 35, 1199–1217, 1999.
- Gelhar, L. W., *Stochastic Subsurface Hydrology*, Prentice-Hall, Old Tappan, N. J., 1993.
- Gupta, V. K., E. Waymire, and C. T. Wang, A representation of an instantaneous unit hydrograph from geomorphology, *Water Resour. Res.*, 16, 855–862, 1980.
- Horton, R. E., Erosional development of streams and their drainage basins: Hydrophysical approach to quantitative morphology, *Geol. Soc. Am. Bull.*, 56, 275–370, 1945.
- Kirkby, M. J., Tests of the random model and its application to basin hydrology, *Earth Surf. Processes Landforms*, 1, 197–212, 1976.
- Kirshen, D. M., and R. L. Bras, The linear channel and its effect on the geomorphologic IUH, *J. Hydrol.*, 65, 175–208, 1983.
- Langhaar, H. L., *Dimensional Analysis and Theory of Models*, 166 pp., Chapman and Hall, New York, 1951.
- Lizarraga, S. P., A nonlinear lumped-parameter model for the Mesilla Valley, New Mexico, M.S. thesis, N. M. Inst. of Min. and Technol., Socorro, N. M., 1978.
- Marani, M., J. Banavar, G. Caldarelli, A. Maritan, and A. Rinaldo, Stationary self-organized fractal structures in an open, dissipative electrical system, *J. Phys. A, Math. Gen.*, 31(18), 337–343, 1998.
- Montgomery, D. R., and W. E. Dietrich, Where do channels begin?, *Nature*, 336, 232–234, 1988.
- Montgomery, D. R., and W. E. Dietrich, Channel initiation and the problem of landscape scale, *Science*, 255, 826–830, 1992.
- Moore, I. D., G. J. Burch, and D. H. MacKenzie, Topographic effects

- on the distribution of surface soil water and the location of ephemeral gullies, *Trans. Am. Soc. Agric. Eng.*, 31, 1098–1107, 1988a.
- Moore, I. D., E. M. O'Loughlin, and G. J. Burch, A contour-based topographic model for hydrological and ecological applications, *Earth Surf. Processes Landforms*, 13, 305–320, 1988b.
- Rasmussen, W. C., and G. E. Anderasen, Hydrologic budget of the Beaverdam Creek Basin, Md., *U.S. Geol. Surv. Water Supply Pap.*, 1472, 106 pp., 1959.
- Rinaldo, A., A. Marani, and R. Rigon, Geomorphological dispersion, *Water Resour. Res.*, 27, 513–525, 1991.
- Rinaldo, A., G. K. Vogel, R. Rigon, and I. Rodriguez-Iturbe, Can one gauge the shape of a basin?, *Water Resour. Res.*, 31, 1119–1127, 1995.
- Rodriguez-Iturbe, I., and A. Rinaldo, *Fractal River Basins: Chance and Self-Organization*, Cambridge Univ. Press, New York, 1997.
- Rodriguez-Iturbe, I., and J. B. Valdes, The geomorphologic structure of the hydrologic response, *Water Resour. Res.*, 15, 1409–1420, 1979.
- Rodriguez-Iturbe, I., M. Gonzales-Sanabria, and R. L. Bras, A geomorphoclimatic theory of the instantaneous unit hydrograph, *Water Resour. Res.*, 18, 877–886, 1982.
- Schicht, R. G., and W. C. Walton, Hydrologic budgets for three small watersheds in Illinois, *Rep. Invest.*, 49, 40 pp., Ill. State Water Surv., Urbana, 1961.
- Senn, R. B., A nonlinear reservoir lumped parameter model for the Herkenhoff farm located near San Acacia, M.S. thesis, N. M. Inst. of Min. and Technol., Socorro, N. M., 1980.
- Snell, J. D., and M. Sivapalan, On geomorphological dispersion in natural catchments and the geomorphological unit hydrograph, *Water Resour. Res.*, 30, 2311–2324, 1994.
- Troch, P. A., F. P. De Troch, and W. Brutsaert, Effective water table depth to describe initial conditions prior to storm rainfall in humid regions, *Water Resour. Res.*, 29, 427–434, 1993.
- Troutman, B. M., and M. R. Karlinger, Unit hydrograph approximations assuming linear flow through topologically random channel networks, *Water Resour. Res.*, 21, 743–754, 1985.
- Tucker, G. E., and R. Slingerland, Drainage basin responses to climate change, *Water Resour. Res.*, 33, 2031–2047, 1997.
- Tucker, G. E., F. Catani, A. Rinaldo, and R. L. Bras, Statistical analysis of drainage density from digital terrain data, *Geomorphology*, 36, 187–202, 2001.
- Yeh, P. J.-F., M. Irizarry, and E. A. B. Eltahir, Hydroclimatology of Illinois: A comparison of monthly evaporation estimates based on atmospheric water balance and soil water balance, *J. Geophys. Res.*, 103, 19,823–19,837, 1998.
- E. Eltahir, Ralph M. Parsons Laboratory, Department of Civil and Environmental Engineering, 48-207, Massachusetts Institute of Technology, Cambridge, MA 02139, USA. (eltahir@mit.edu)
- M. Marani and A. Rinaldo, Dipartimento di Ingegneria Idraulica, Marittima e Geotecnica, Università di Padova, via Loredan 20, I-35131 Padova, Italy. (rinaldo@idra.unipd.it)

(Received November 28, 2000; revised May 7, 2001; accepted May 7, 2001.)